ANALYSIS OF THE INFLUENCE OF OPERATING CONDITIONS AND GEOMETRIC PARAMETERS ON THERMAL CHARACTERISTICS OF LOW TEMPERATURE N-OCTADECANE LATENT HEAT STORAGE

Fouzi Benmoussa[1],
Hocine Benmoussa[1],
Ahmed Benzaoui[2].

[1]Faculty of Technology, Mechanics Department, University of Batna-2- Batna, Algeria
[2]Faculty of Physics, University of Houari Boumedienne Sciences and Technology, Algiers, Algeria
E-mail : benmoussa_fouzi@yahoo.fr ; hocine_b@hotmail.com ; a1benzaoui@yahoo.fr

ABSTRACT

This work presents a numerical study of the thermal characteristics of low temperature n-octadecane latent heat storage unit (LHSU) in a shell-and-tube configuration. Phase change material (PCM) is filled in the shell space. The heat transfer fluid (HTF) flow through the tube and transfer the heat to PCM. First, a mathematical model is developed based on the enthalpy formulation and solved through the governing equations for different parameters. Second, the effects of Stefan and Reynolds number on the unsteady temperatures evolution of PCM as well as the unsteady total energy stored evolution are studied. Third, some operating conditions and geometric parameters are then undertaken to assess the effects of HTF inlet temperature, HTF inlet velocity and inner tube radius on melting time. The results show that charging process has three periods for the change of temperature regarding to time in PCM: rapidly changing period, no changing period and slowly changing period. The total energy stored gradually increases from minimum value which define the beginning of the charging process to maximum value defined the end of the process. The effects of Stefan number on the total energy stored show that heat storage capacity is large for high Stefan number. The Reynolds number has little influences on the amount of total energy stored, except the time needed for completing charging process. The results show also that within the studied parameters, the HTF inlet temperature has the largest effect on LHSU rate. With HTF inlet temperature increasing from 302.7K to 325.7K, the melting time reduces 92%. The second influential factor is the HTF inlet velocity. When inlet velocity increases from 0.01m/s to 0.6m/s, the melting time reduces 32%. Tube radius has the lowest effect. With inner tube radius increasing from 6.35mm to 50 mm, the melting time augments 49%. Results show that these operating conditions and geometric parameters must be chosen carefully in order to optimize the thermal performance of the LHSU.

KEY WORDS

- Latent heat storage,
- Phase change material,
- Double concentric tube,
- Total energy stored,
- Melting time,
- Sensible heat,
- Latent heat.

NOMENCLATURE

A, B Representative location inside PCM
a Convective heat transfer coefficient (W.m^{-2}K^{-1})
C_p Specific heat (J.kg^{-1}K^{-1})
D_1 Diameter of the inner tube (m)
E Total energy stored (J.kg^{-1})
f PCM melting fraction
k Thermal conductivity (W.m^{-1}K^{-1})
L Length of the tube (m)
M Number of axial nodes
m Mass of the PCM (Kg)
N Number of radial nodes
Q_m Mass flow rate (Kg.s^{-1})
R_1 Inner tube radius (m)
R_2 Outer tube radius (m)
r Coordinate along the radial direction (m)
T Temperature (K)
t Time (s)
U Velocity (m.s^{-1})
x Coordinate along the axial direction (m)

Greek symbols
μ Dynamic viscosity (Kg.m^{-1}s^{-1})
ρ Density (Kg.m^{-3})
ΔH Latent heat of fusion (kJ.kg^{-1})
θ Relative temperature (K)

Abbreviations
HTF Heat transfer fluid
$LHSU$ Latent heat storage unit
PCM Phase change material

Dimensionless
Re Reynolds number, $4Q_m/\pi D_1 \mu_f$
Ste Stefan number, $C_p(T_{in} - T_M)/\Delta H$

Subscripts
f Heat transfer fluid
M Melting temperature
pcm Phase change material
In Inlet boundary
Ini Initial condition

6

ANALYSIS OF THE INFLUENCE OF OPERATING CONDITIONS AND GEOMETRIC PARAMETERS ON THERMAL CHARACTERISTICS OF LOW TEMPERATURE N-OCTADECANE LATENT HEAT STORAGE

1. INTRODUCTION

These last years, the deterioration of energy crisis, the environmental pollution and global warming are strongly increased the interest in utilizing renewable energy sources, especially solar energy. In order to relieve this situation to some extent, a lot of efforts and researches on solar thermal utilizations have been carried out. These efforts include solar buildings [1-2], solar water heating systems [3-4] and solar energy generation systems [5-6]. However, solar energy has a shortcoming that it is unstable and discontinuous with different weathers, times and seasons. To ensure the solar energy system operations continuously and stable with high efficiency, thermal energy storage have become a necessary component. The main objective is then to eliminate the mismatch between energy supply and energy demand. Latent heat storage unit (LHSU) with solid-liquid phase change has become a subject of increasing attention over the past decade. The importance of phase change materials (PCMs) for heat storage is well recognized, due mainly to their high thermal storage density and heat charging/discharging at a nearly constant temperature. The shell-and-tube LHSU is currently the most widely used one of thermal storage modes. In the shell-and-tube LHSU, the heat is transferred from heat transfer fluid (HTF) which flows in the tube to PCM which is filled in the shell space and the heat is stored or released by the melting or solidification of PCM. Many studies concerning the thermal characteristics of shell-and-tube LHSU based on different types of PCMs have been undertaken : Trp et al. [7-8] established a mathematical model to analyze the transient heat transfer phenomena of melting and solidification of paraffin wax in a cylindrical shell. They concluded that the operating conditions and geometric parameters should be chosen carefully to optimize the thermal performance of the storage unit. Wang et al. [9], Lacroix [10] numerically and experimentally studied the effects of temperature difference between HTF inlet temperature and melting point of PCM, the HTF inlet mass flow rate on heat charging and discharging performance.

2. MODEL DESCRIPTION AND MATHEMATICAL FORMULATIONS

2.1. Physical model

The schematic representation of the LHSU is shown in Figure 1a, which is similar to the model used by Wang et al. [9] and Lacroix [10]. The physical model to be analysed is represented by a simple geometry shown in Figure 1b. The LHSU is a shell-and-tube configuration. The HTF flows in the inner tube, and the shell side is full of PCM (n-octadecane). The thermo-physical properties of PCM and HTF are shown in Table 1. The length for the computation domain (L) is 1 m, the radius for the inner tube (R1) is

The layout of the phase change storage unit considered consists of a shell-and-tube type. The annulus space is filled with PCM (n-octadecane). The results show that HTF inlet temperature has great effect on the time to complete heat charging or discharging cycles, at the same time more energy is stored for higher HTF inlet temperature. Adine and Qarnia [11] presented a numerical study of LHSU consisting of a shell-and-tube. Two PCMs were filled in the shell space, and water flowed through the inner tube to transfer heat with PCMs. Several numerical investigations were conducted in order to compare the thermal performance of the unit using two PCMs and a single PCM. Akgun et al. [12-13] analyzed the LHSU of the shell-and-tube type with three kinds of paraffin as PCMs. A novel tube-in-shell storage geometry was introduced and the effects of Reynolds and Stefan numbers on melting and solidification behaviors were examined. Kibria et al. [14] numerically and experimentally investigated a thermal storage unit of phase change process dominated by heat conduction. The thermal energy storage involves a shell-and-tube, where paraffin wax as PCM is filled in the shell. Experimental setup has been designed and built to examine the physical validity of the numerical results. Graphical representation of different results including the outlet temperature of HTF versus time, solid–liquid interface versus axis position of PCM and heat transfer versus time is presented and discussed.

In the present study, in order to investigate the performance and thermal characteristics of low temperature LHSU under variable conditions, a physical and mathematical model was established for the shell-and-tube LHSU with n-octadecane as PCM and water as HTF. The simulation for the LHSU process was based on the enthalpy method which takes into account phase change phenomenon. Numerical simulations are carried out to investigate the effects of Stefan and Reynolds numbers on the unsteady temperatures evolution of PCM as well as the unsteady total energy stored evolution. The effects of HTF inlet temperature, HTF inlet velocity and inner tube radius on melting time are also presented.

6.35 mm, and the radius for the shell side (R2) is 12.9 mm. The PCM having melting temperature 300.7 K is a suitable material used to store heat energy produced by domestic solar water heating system. In charging process, initially the PCM is solid; its temperature is set to 282.7 K. In such system the HTF inlet temperature ranges from 302.7 K to 325.7 K. Thus, the temperature difference between the inlet of HTF and melting point of PCM range from +2 K to +25 K. For the HTF, it is a general view that the HTF flow in the tube should be less than 1 m/s to obtain a good performance. Thus, the mass flow rates range from 0.00125 kg/s to 0.075 kg/s, which correspond to water velocity ranging from 0.01 m/s to 0.6 m/s, is chosen in present study.
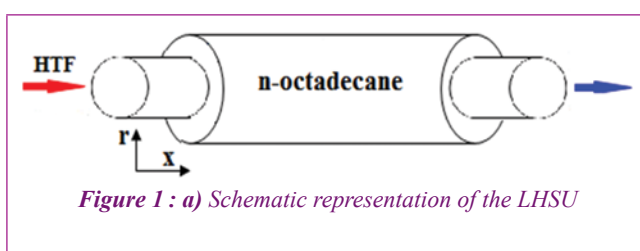
Figure 1 : a) Schematic representation of the LHSU
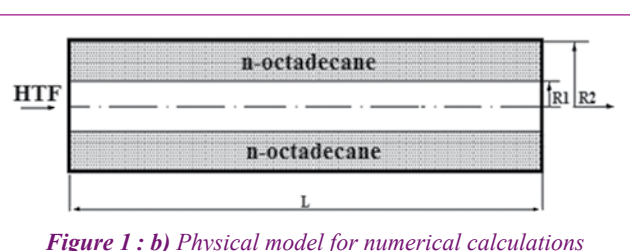
Figure 1 : b) Physical model for numerical calculations

ANALYSIS OF THE INFLUENCE OF OPERATING CONDITIONS AND GEOMETRIC PARAMETERS
ON THERMAL CHARACTERISTICS OF LOW TEMPERATURE N-OCTADECANE LATENT HEAT STORAGE

7

Table 1. Thermo-physical properties of n-octadecane and water [9-10]

	n-octadecane	**water (T = 310.7 K)**
Fusion temperature, (K)	300,7	/
Latent heat of fusion, (kJ.kg^{-1})	243,5	/
Thermal conductivity, (W.m^{-1}.K^{-1})	0,358	0,628
Specific heat, (J.kg^{-1}K^{-1})	2222	4178
Density, (kg.m^{-3})	771	993
Dynamic viscosity, (kg.m^{-1}.s^{-1})	3,107.10^{-3}	695.10^{-6}

2.2. Assumptions

In order to simplify the physical and mathematical model, the following assumptions are adopted.
- The flow is Newtonian, incompressible and fully developed dynamically ;
- The HTF flow is laminar, inlet velocity and inlet temperature of the HTF are both constant ;
- The viscous dissipation in the HTF is neglected. HTF is treated as one dimensional fluid flow along the tube axial direction ;

- The thermo-physical properties of the PCM are independent of temperature ;
- The thermo-physical properties of solid and liquid phases of PCM are equal ;
- The effect of liquid PCM natural convection is neglected ;
- The thickness of tube wall is neglected ;
- The outer surface of the shell side is treated as an adiabatic boundary ;
- The problem is axisymmetric.

2.3. Mathematical formulations

Based on the above assumptions, the LHSU process in the shell-and-tube unit can be treated as an axisymmetric model. The enthalpy method is used to deal with the moving boundary problem in PCM melting process. The governing equations for the HTF and PCM region are shown as follows :

- For the HTF region

$$\left(\rho C_p\right)_{pcm} \frac{\partial \theta_{pcm}(x,r,t)}{\partial t} = k_{pcm}\left[\frac{\partial^2 \theta_{pcm}(x,r,t)}{\partial x^2} + \frac{1}{r}\frac{\partial}{\partial r}\left(r\frac{\partial \theta_{pcm}(x,r,t)}{\partial r}\right)\right] - \rho_{pcm}\Delta H \frac{\partial f}{\partial t} \quad \text{......} (1)$$

$$x > 0 \,,\, 0 < r < R_1 \,,\, t > 0$$

Where ρ is the density of fluid, C_p is the specific heat, U is the fluid velocity, and k is the thermal conductivity.

- For the PCM region

$$\left(\rho C_p\right)_{pcm} \frac{\partial \theta_{pcm}(x,r,t)}{\partial t} = k_{pcm}\left[\frac{\partial^2 \theta_{pcm}(x,r,t)}{\partial x^2} + \frac{1}{r}\frac{\partial}{\partial r}\left(r\frac{\partial \theta_{pcm}(x,r,t)}{\partial r}\right)\right] - \rho_{pcm}\Delta H \frac{\partial f}{\partial t} \quad \text{......} (2)$$

$$x > 0 \,,\, R_1 < r < R_2 \,,\, t > 0$$

f is the PCM melting fraction; the melting fraction during charging process is determined as :

$$\begin{cases} f = 0, & \theta < 0 & Solid \\ 0 < f < 1, & \theta = 0 & Solid + Liquid \\ f = 1, & \theta > 0 & Liquid \end{cases} \quad \text{......} (3)$$

Where $\theta = (T - T_M)$

The Eq. (2) is formulated by using the enthalpy method (Voller [15]), in which the total enthalpy is split into sensible heat and latent heat :

$$H(T) = h(T) + \rho f \Delta H \quad \text{......} (4)$$

Where $h(T) = \int_{T_M}^{T} \rho C_p \, dT \quad \text{......} (5)$

2.4. Initial and boundary conditions

- **Initial conditions**

For the HTF region :

$$\begin{cases} T_f\left(x, 0 < r < R_1, t = 0\right) = T_{ini} \\ U_f\left(x, 0 < r < R_1, t = 0\right) = U_{ini} \end{cases} \quad \text{......} (6a)$$

For the PCM region :

$$T_{pcm} = (x, R_1 \leq r \leq R_2, t = 0) = 282,7\,K \quad \text{......} (6b)$$

- **Boundary conditions**

For the HTF region :

$$\begin{cases} U_f(0,r,t) = U_{f,in} \\ T_f(0,r,t) = T_{f,in} \end{cases} \quad 0 < r < R_1 \,,\, t > 0 \quad \text{......} (7a)$$

$$\left.\frac{\partial U_f(x,r,t)}{\partial r}\right|_{r=0} = \left.\frac{\partial T_f(x,r,t)}{\partial r}\right|_{r=0} = 0 \quad x > 0, t > 0 \quad \text{......} (7b)$$

For the PCM region :

$$\left.\frac{\partial T_{pcm}(x,r,t)}{\partial r}\right|_{r=R_2} = 0 \quad x > 0, t > 0 \quad \text{......} (7c)$$

$$\left.\frac{\partial T_{pcm}(x,r,t)}{\partial x}\right|_{x=0} = \left.\frac{\partial T_{pcm}(x,r,t)}{\partial x}\right|_{x=L} = 0 \quad \text{......} (7d)$$

$$R_1 < r < R_2, t > 0$$

At the inner surface boundary :

$$a_f \left(T_f - T(x, r = R_1, t) \right) = - k_{pcm} \left. \frac{\partial T_{pcm}(x, r, t)}{\partial r} \right|_{r = R_1}$$

$$x > 0 \, , \, r = R_1 \, , \, t > 0 \qquad \text{...... (7e)}$$

Where a_f is local convective heat transfer coefficient (W.m^{-2}.K^{-1}).

Before we proceed to the next section, we introduce two fundamental dimensionless numbers : the Reynolds and the Stefan number :

$$Re = \frac{4 Q_m}{\pi D_1 \mu_f} \, , \quad Ste = \frac{Cp_{pcm}(T_{in} - T_M)}{\Delta H} \qquad \text{...... (8)}$$

Where Q_m is the mass flow rate of HTF, D_1 is the inner tube diameter, μ_f is the dynamic viscosity, C_p is the specific heat of PCM, T_{in} is the inlet temperature of HTF, T_M is the PCM melting temperature and ΔH is the latent heat of fusion.

The total energy stored during charging process can be represented by the following expression :

$$E = \int_{T_{pmc}}^{T_M} m \, C_p \, dT + m f \Delta H + \int_{T_{pmc}}^{T_f} m \, C_p \, dT \qquad \text{...... (9)}$$

$$E = m C_p (T_M - T_{pcm}) + m f \Delta H + m C_p (T_f - T_{pcm}) \qquad \text{...... (10)}$$

The first term of the Eq. (10) represents the sensible heat charging period, when the PCM temperature increase from its initial temperature to the phase change, the second term represents the latent heat charging during the phase change period. The third term represents the second sensible heat charging period under a fusion form until reaching the steady state.

3. NUMERICAL SOLUTION

Commercial CFD program FLUENT 6.3 was used to conduct the numerical calculations, where the finite volume method described by Patankar [16] was used. The energy equations were discretized with the first order upwind scheme. The time integration has been performed fully implicitly and control volumes of a uniform size and constant time steps were used.

3.1. Selection of grid size

In order to use an optimum grid size that guarantee the accuracy requirement and computing cost, three different grid sizes with quadrilateral cells were tested under the same working conditions (100×20), (100×30) and (100×40). The three grid resolutions are evaluated under HTF inlet temperature 305.7 K. The results of the variation of temperature respecting to time at location A (x=0.51, r=0.0099) m under the three different grid sizes are shown in Figure 2. As shown in the figure, the relative solution deviations with the three different grid sizes are very remarkable. The grid sizes of (100×30) and (100×40) shows some perturbations during the numerical tests, on the other hand, the temperature evolution of PCM under the grid size (100×20) is very stable from the stars of heating until the end of charging process. The grid size of (M=100×N=20) can be regarded as a grid size through which grid independent results can be obtained.
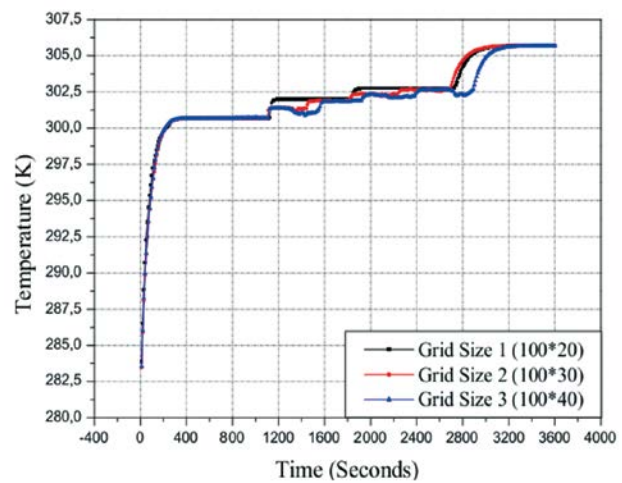
Figure 2) PCM temperature versus time for different grid sizes.

3.2. Model validation

The physical model and simulation code was verified with experimental data obtained by Lacroix [10], were investigated under the same operating conditions and geometric parameters. Charging process was studied experimentally under two different HTF inlet temperatures : $T_{f,in} = 305,7 \, K$ and $T_{f,in} = 310.7 \, K$, the HTF inlet velocity was maintained constant during the test. The comparison between numerical results and experimental data has been presented in terms of temperature evolution of PCM at location $A(x = 0,51 \, ; \, r = 0,0099) \, m$. As shown in Figures 3 and 4, the numerical results are in good agreement with experimental data. These results indicate that the present computational model can be used for investigating the thermal characteristics of n-octadecane latent heat storage unit under different physical and geometrical parameters.
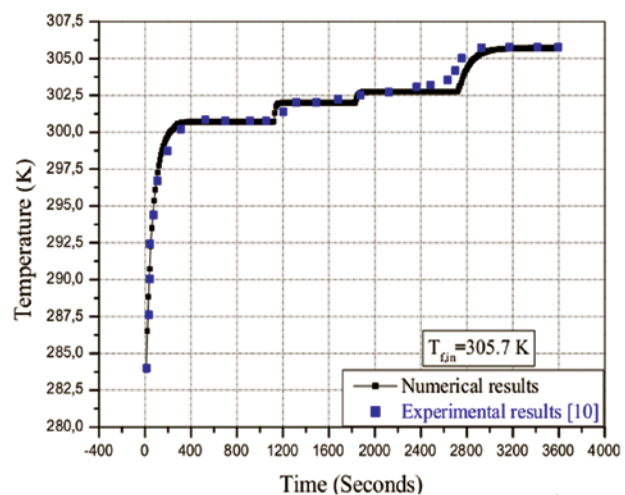
Figure 3) Comparison results between numerical simulation and experiment data, $T_{f,in} = 305,7 \, K$.

ANALYSIS OF THE INFLUENCE OF OPERATING CONDITIONS AND GEOMETRIC PARAMETERS
ON THERMAL CHARACTERISTICS OF LOW TEMPERATURE N-OCTADECANE LATENT HEAT STORAGE

9
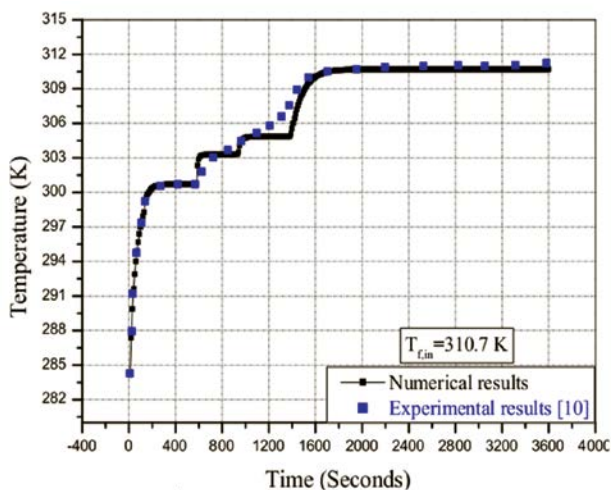
Figure 4) *Comparison results between numerical simulation and experiment data, $T_{f,in}$ = 310.7 K.*

4. NUMERICAL RESULTS AND DISCUSSIONS

The main objective of our numerical simulations is to give an idea about the thermal characteristics and behaviour of the LHSU during charging process. The temperature evolution at location B $(x = 0,25 ; r = 0,007)$ m as well as the unsteady total energy stored evolution in PCM under different value of Stefan and Reynolds number are investigated. The effects of HTF inlet temperature, HTF inlet velocity and inner tube radius on melting time has also presented. The detailed results will be presented and discussed in the following sections.

4.1. Unsteady temperature evolutions of PCM

Melting of the PCM, i.e., the storing of thermal energy, has been first observed. The n-octadecane was initially in the solid phase; its temperature is set to *282,7 K*. Analysis has been performed for three different HTF inlet temperatures above the melting point of the PCM (*305,7 K*, *310,7 K* and *320,7 K*) and the Stefan number, which represents the ratio of the PCM sensible and latent heat, corresponding respectively to $Ste = 0,045, 0,091$ and $0,182$. The HTF inlet velocity has been *0,01 m/s*, *0.05 m/s* and *0,15 m/s*, corresponding respectively to $Re = 164, 821$ and 2464.

Figures 5 and **6** shows the variation of temperature respecting to time at location B during charging process, under three different value of Stefan and Reynolds number, respectively. The thermal behaviour of the LHSU presents three distinct periods. During the first period, the PCM temperature increases rapidly from the start of heating process to the beginning of the phase change, the material stores energy primarily by sensible heat. During the second period, the energy is mainly charged by latent heat, and the temperature evolution of PCM keeps constant. The third period starts when all PCM is melted, during this period, the PCM temperature starts to increase slowly until reaching the value of the HTF inlet temperature, the energy is charged only by sensible heat under a fusion form until reaching the steady state. Its observed that the second period (period when energy is mainly charged by latent heat) is shorter when the Stefan number increase from *0,045* to *0,182*, also when

the Reynolds number increase from *164* to *2464*. The increasing of Stefan and Reynolds number leads to the increase in heat transfer rate between HTF and PCM, which make the melting time shorter. The effects of Stefan number is very remarkable than the effects of Reynolds number in term of melting time.
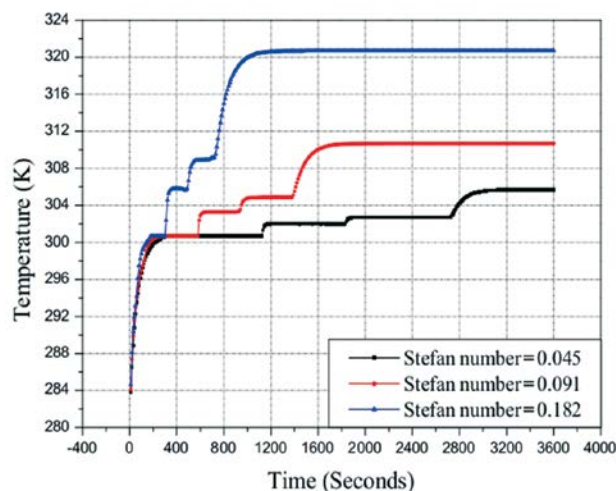
Figure 5) *PCM temperature versus time under different value of Stefan number.*
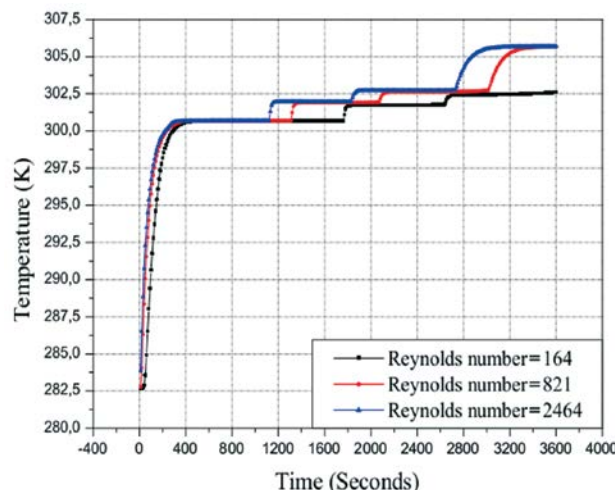
Figure 6) *PCM temperature versus time under different value of Reynolds number.*

Figure 7 shows the effect of Stefan number on the total energy stored evolutions. As shown in the figure, when the Stefan number increases from *0,045* to *0,182*, the thermal energy carried by the HTF enhances, then, the heat transmitted to the PCM becomes important and the charging process is rapidly reached. Hence, the total energy stored gradually increases from minimum value which define the beginning of the first sensible heat charging to maximum value defined the end of the second sensible heat charging. The total energy stored reaches its maximum value, then remains constant and equals *260000 J/kg*, *271000 J/kg* and *293000 J/kg* for Stefan number *0,045*, *0,091* and *0,182*, respectively. These results show that heat storage capacity is large for high Stefan number, which define the high temperature difference between HTF inlet temperature and melting point of PCM.

ANALYSIS OF THE INFLUENCE OF OPERATING CONDITIONS AND GEOMETRIC PARAMETERS ON THERMAL CHARACTERISTICS OF LOW TEMPERATURE N-OCTADECANE LATENT HEAT STORAGE

Figure 8 shows the effect of Reynolds number on the total energy stored evolutions. The HTF inlet temperature was maintained constant during the tests to a value of *310,7 K*. As shown in the figure, for all values of Reynolds number, the total energy stored gradually increases from minimum value to maximum value defined the end of the charging process. The total energy stored reaches its maximum value, then remains constant and equals *271000 J/kg* for all values of Reynolds number. Reflected in the figure, for all numerical tests, the Reynolds number has little influences on the amount of energy stored, except the time needed for completing the charging process.
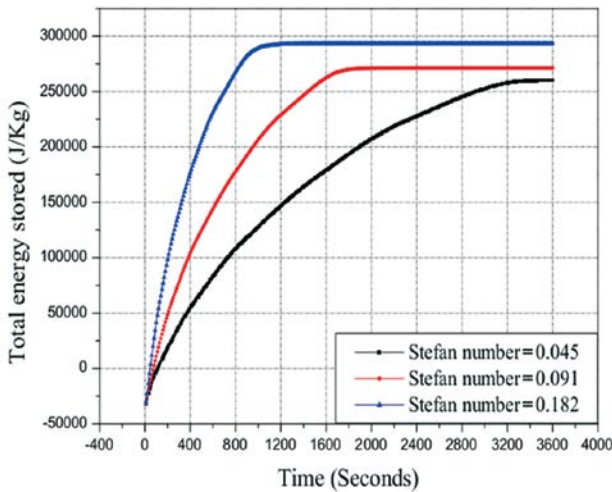
Figure 7) Total energy stored versus time under different value of Stefan number.
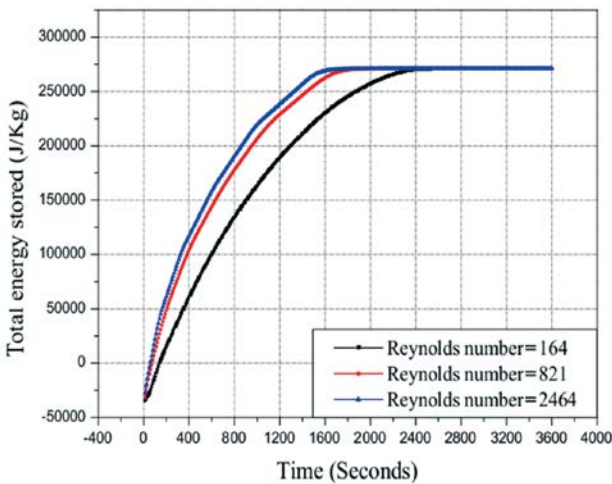
Figure 8) Total energy stored versus time under different value of Reynolds number.

4.3. Effects of HTF inlet temperature, HTF inlet velocity and inner tube radius on melting time

The effects of HTF inlet temperature on the PCM melting time for different value of HTF inlet velocity are shown in **Figure 9**. With the HTF inlet temperature increase, the temperature difference between HTF and PCM augments, which causes the heat transfer rate increasing. So, the PCM melting time reduces. For HTF inlet velocity *0,15 m/s*, when HTF inlet temperature increases from *302,7 K* to *325,7 K*, the melting time reduces from *110,83 min* to *9,83 min*, which reduces about 90%. So,

increasing the HTF inlet temperature can efficiently reduce the melting time.

The effects of HTF inlet velocity on the PCM melting time for different value of HTF inlet temperature are shown in **Figure 10**. With the HTF inlet velocity increase, the convection heat transfer coefficient is augmented, which leads to the heat transfer rate between HTF and PCM increase. So, the PCM melting rate is accelerated and the melting time is reduced. For HTF inlet temperature *310,7 K*, when HTF inlet velocity increases from *0,01 m/s* to *0,6 m/s*, the melting time reduces from *32,66 min* to *22,50 min*, which reduces about 32%. So, increasing the HTF inlet velocity can obviously reduce the melting time. Its observed from **Figures 9** and **10**, the effects of HTF inlet temperature is very remarkable than the effects of HTF inlet velocity in term of melting time. **Figure 11** shows the effects of inner tube radius on melting time. During the numerical tests we keep $(R_2 - R_1 = 6,55\ mm)$, the mass flow rate for HTF was maintained constant. It can be seen, with the inner tube radius increase, the melting time augments. Due to the increase in the cross section, the HTF velocity decrease and the heat transfer rate is weakened. When inner tube radius increases from *6,35 mm* to *50 mm*, melting time increases from *23 min* to *46,83 min*, which augments about 49%.
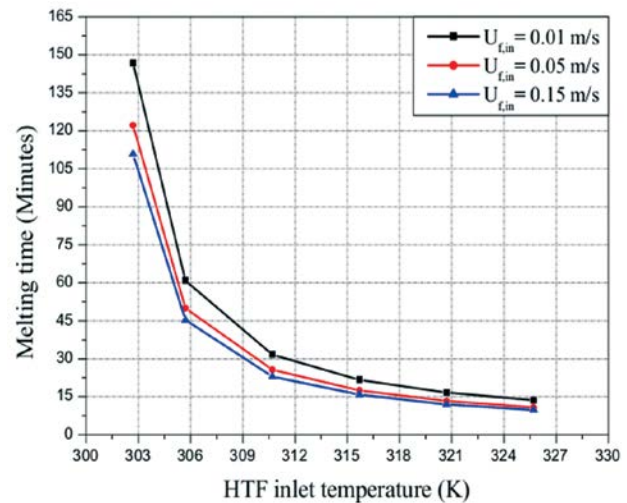
Figure 9) Effects of HTF inlet temperature on melting time.
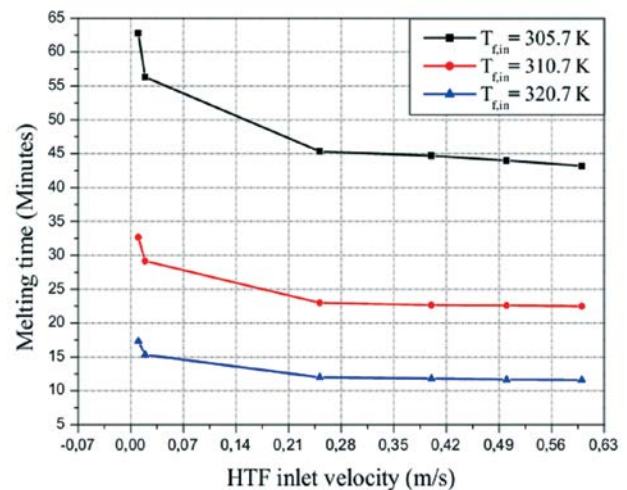
Figure 10) Effects of HTF inlet velocity on melting time.

ANALYSIS OF THE INFLUENCE OF OPERATING CONDITIONS AND GEOMETRIC PARAMETERS ON THERMAL CHARACTERISTICS OF LOW TEMPERATURE N-OCTADECANE LATENT HEAT STORAGE

11
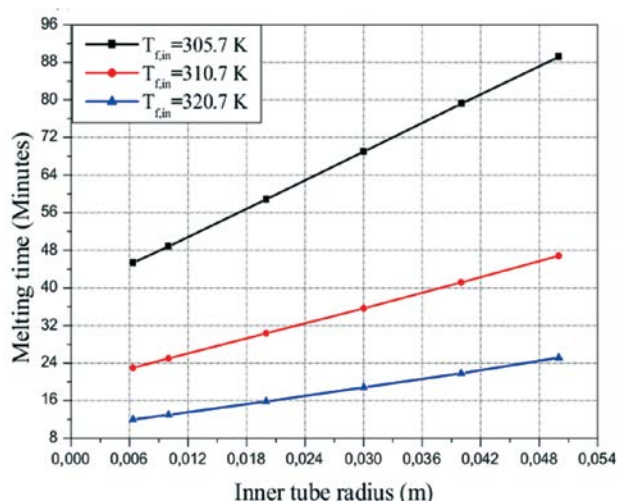
Figure 11) Effects of inner tube radius on melting time.

5. CONCLUSION

In the present paper, in order to reveal the thermal characteristics of low temperature n-octadecane LHSU under different operating conditions and structural parameters, a mathematical model formulated in two-dimensional cylindrical coordinates based on the enthalpy formulation has been presented. The effects of Stefan and Reynolds number on the PCM temperature evolution as well as the total energy stored evolution are studied. The effects of HTF inlet temperature, HTF inlet velocity and inner tube radius on melting time (time required for PCM completely melting) were also numerically investigated. According to the results and discussions, the following conclusions can be derived :

- Under all operating conditions and structural parameters, charging process has three periods for the change of temperature regarding to time in PCM : rapidly changing period, no changing period and slowly changing period.

- The increasing in Stefan and Reynolds number leads to the increase in heat transfer rate between HTF and PCM, which make the melting time shorter ; the effects of Stefan number is very remarkable than the effects of Reynolds number in term of melting time.

- Heat storage capacity is large for high Stefan number, which define the high temperature difference between HTF inlet temperature and melting point of PCM.

- The Reynolds number has little influences on the amount of energy stored, except the time needed for completing the charging process.

- When HTF inlet temperature increases from *302,7 K* to *325,7 K*, the melting time reduces from *110,83 min* to *9,83 min*, which reduces about 90%.

- When HTF inlet velocity increases from *0,01 m/s* to *0,6 m/s*, the melting time reduces from *32,66 min* to *22,50 min*, which reduces about 32%.

- When inner tube radius increases from *6,35 mm* to *50 mm*, the melting time increases from *23 min* to *46,83 min*, which augments about 49%.

REFERENCES

[1] InW. Xiao, X. Wang and Y.P. Zhang, Analytical optimization of interior PCM for energy storage in a light weight passive solar room, Applied Energy, 86 (2009) 2013-2018.

[2] F. Kuznik and J. Virgone, Experimental assessment of a phase change material for wall building use, Applied Energy, 86 (2009) 2038-2046.

[3] C. Garnier, J. Currie and T. Muneer, Integrated collector storage solar water heater: temperature stratification, Applied Energy, 86 (2009) 1465-1469.

[4] K. Sutthivirode, P. Namprakai and N. Roonprasang, A new version of a solar water heating system coupled with a solar water pump, Applied Energy, 86 (2009) 1423-1430.

[5] Z. Yang and S.V. Garimella, Molten-salt thermal energy storage in thermoclines under different environmental boundary conditions, Applied Energy, 87 (2010) 3322-3329.

[6] Y.B. Tao and Y.L. He, Numerical study on coupled fluid flow and heat transfer process in parabolic trough solar collector tube, Solar Energy, 84 (2010) 1863-1872.

[7] A. Trp, An experimental and numerical investigation of heat transfer during technical grade paraffin melting and solidification in a shell-and-tube latent thermal energy storage unit, Solar Energy, 79 (2005) 648-660.

[8] A. Trp, K. Lenic, and B. Frankovic, Analysis of the influence of operating conditions and geometric parameters on heat transfer in water-paraffin shell-and-tube latent thermal energy storage unit, Applied Thermal Engineering, 26 (2006) 1830-1839.

[9] W.W Wang, K. Zhang, L.B. Wang and Y.L. He, Numerical study of the heat charging and discharging characteristics of a shell-and-tube phase change heat storage unit, Applied Thermal Engineering, 58 (2013) 542-553.

[10] M. Lacroix, Numerical simulation of a shell-and-tube latent heat thermal energy storage unit, Solar Energy, 50 (1993) 357-367.

[11] H. A. Adine and H. E. Qarnia, Numerical analysis of the thermal behavior of a shell-and-tube heat storage unit using phase change materials, Applied Mathematical Modelling, 33 (2009) 2132-2144.

[12] M. Akgun, O. Aydin and K. Kaygusuz, Experimental study on melting/solidification characteristics of a paraffin as PCM, Energy Conversion and Management, 48 (2007) 669-678.

[13] M. Akgun, O. Aydin and K. Kaygusuz, Thermal energy storage performance of paraffin in a novel tube-in-shell system, Applied Thermal Engineering, 28 (2008) 405-413.

[14] M.A. Kibria, M.R. Anisur, M.H. Mahfuz, R. Saidur and I.H.S.C. Metselaar, Numerical and experimental investigation of heat transfer in a shell-and-tube thermal energy storage system, International Communications in Heat and Mass Transfer, 53 (2014) 71–78.

[15] V.R. Voller, Fast implicit finite-difference method for the analysis of phase change problems, Numerical Heat Transfer, 17 (1990) 155-169.

[16] S.V. Patankar, Numerical Heat Transfer and Fluid Flow, Hemisphere Publishing Corporation, New York, 1980.

12

ANALYSIS OF THE INFLUENCE OF OPERATING CONDITIONS AND GEOMETRIC PARAMETERS ON THERMAL CHARACTERISTICS OF LOW TEMPERATURE N-OCTADECANE LATENT HEAT STORAGE